# Uplink Capacity Analysis of OFDMA Based Cellular Networks with Reuse-1

Maciej Mühleisen, Daniel Bültmann, Bernhard Walke
ComNets Research Group
Faculty 6, RWTH Aachen University, Germany
Email: {mue|dbn|walke}@comnets.rwth-aachen.de

***Abstract*—OFDMA based cellular radio networks aim to operate as close as possible to frequency reuse distance of one, where the whole spectrum would be available in every cell. Modern systems are able to adjust parameters such as transmission power, modulation, and coding separately for each frequency sub-channel on a very short time scale. This way Fractional Frequency Reuse (FFR) can be applied, allowing to operate reuse-1 in the center of cells and reuse greater one at cell edges. This paper presents a novel method to analyze the Carrier to Interference Ratio (CIR) distribution and uplink capacity of a cell, from which spectral efficiency of a cellular radio network using FFR is derived. The results presented apply for OFDMA cellular networks operated in IMT-Advanced evaluation scenarios.**

## I. Introduction

A key goal in today's wireless radio network deployments is maximum spectral efficiency, which can be achieved by applying an optimum frequency reuse distance. This way the bandwidth available to each cell is optimized. Assignment of the whole frequency bandwidth to every cell, would result in reuse distance of one. It is known however, that reuse-1 deployments suffer from low performance at the cell edge, owing to a low Carrier to Interference Ratio (CIR) at terminal receivers.

Future radio access technologies like the IMT-Advanced (IMT-A) candidate systems IEEE 802.16m (WiMAX-A) [1] and 3GPP Long Term Evolution Advanced (LTE-A) [2] are based on Orthogonal Frequency Division Multiple Access (OFDMA) transmission, opening up a high degree of freedom on how radio resources are scheduled in time and frequency domains. With OFDMA, sub-channels formed of multiple sub-carriers can be scheduled with different transmission powers and Modulation and Coding Schemes (MCSs) within a time scale of a few micro seconds. By applying mutable power masks, Fractional Frequency Reuse (FFR) [3] can be achieved, compensating the low CIR experienced by cell edge users, adequately.

With FFR different subsets of frequency sub-channels are operated with different powers, depending on the distance of terminals from the cell center. In this work we evaluate a specific FFR configuration referred to as *Partial Frequency Reuse (PFR)* [4]. More advanced FFR approaches like Soft Frequency Reuse (SFR) [5], [6] could also be analyzed using the method introduced in this paper. With PFR a subset of the available bandwidth is reserved for cell edge users and distributed among cells in a conventional reuse three pattern. In the following we refer to these sub-channels as the *edge band*. The remaining bandwidth is used in the cell center in every cell, leading to a reuse distance of one. We refer to that sub-channel set as *center band*. Figure 1 shows such a configuration with a center cell and two tiers of surrounding cells.

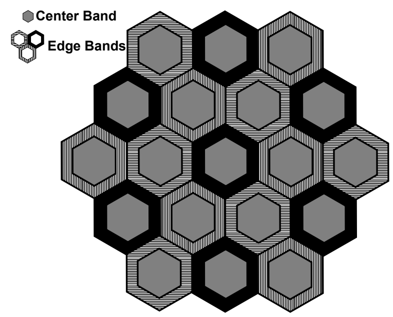


Fig. 1. PFR scenario with reuse-1 in the cell centers and reuse-3 at the cell edges.

### A. IMT-Advanced Evaluation Methodology

The International Telecommunication Union (ITU) has published the IMT-A Circular Letter to specify and evaluate mobile radio networks of the 4th generation. Among others, high spectral efficiency is one of the key goals for such systems. The IMT-A Evaluation Methodology [7] document defines scenarios, where candidate systems have to prove their ability to meet the performance requirements specified, namely hexagonal cellular deployments for Urban Micro (UMi), Urban Macro (UMa), Suburban Macro (SMa), and Rural Macro (RMa) scenarios. Each scenario is characterized by its inter-site distance $D$, User Terminal (UT) class distribution, and channel model parameters. UT class can be outdoor, indoor or in-car. The channel model consists of a large- and a small time scale fading model. In the following only the large scale model for outdoor UTs is explained and used for the analysis presented later. The model specifies the path-loss at a given distance to have both, a fixed and a random component. Parameters differ whether line-of-sight (LoS) or non line-of-sight (NLoS) channel conditions apply. The channel condition is chosen randomly from a distribution that depends on the distance to the transmitter. The shorter the distance, the higher the LoS probability. The received power (in dBm) at distance $d$ is $P_{TX} - (\beta + \gamma \ln d)$. The parameters for the different scenarios and channel conditions are given in Table I. $P_{TX}$ is the transmission power which is limited to 24 dBm for the Uplink (UL). The natural logarithm is chosen to avoid correction factors in the equations presented later. The random component of the path-loss model is log-normally distributed shadow fading, which is added to the distance dependent fixed path-loss. Equation (1) gives the distribution of received power without antenna gains at distance $d$.

TABLE I
IMT-ADVANCED EVALUATION PATH-LOSS MODEL PARAMETERS

| Scenario | $\beta$ [dB] | $\gamma$ | $\sigma$ [dB] |
|---|---|---|---|
| UMi LoS $d < 150$ m | 35.96 | 9.55 | 3 |
| UMi LoS $d \geq 150$ m | $-3.16$ | 17.37 | 3 |
| UMi NLoS | 19.46 | 18.80 | 4 |
| UMa LoS $d < 320$ m | 34.02 | 9.55 | 4 |
| UMa LoS $d \geq 320$ m | $-11.02$ | 17.37 | 4 |
| UMa NLoS | 19.56 | 16.98 | 6 |
| SMa LoS $d < 453.33$ m | 36.15 | 9.37 | 4 |
| SMa LoS $d \geq 453.33$ m | $-12.79$ | 17.37 | 6 |
| SMa NLoS | 12.26 | 16.78 | 8 |
| RMa LoS $d < 181.33$ m | 29.80 | 8.89 | 4 |
| RMa LoS $d \geq 181.33$ m | $-14.28$ | 17.37 | 6 |
| RMa NLoS | 3.99 | 16.98 | 8 |

$$p(x|d) = \frac{1}{\sqrt{2\pi}\sigma} e^{-\frac{(x-(P_{TX}-(\beta+\gamma \ln d)))^2}{2\sigma^2}} \tag{1}$$

The standard deviation $\sigma$ of the normal distribution depends on scenario and channel condition as provided by Table I.

The IMT-A Evaluation Methodology specifies three dimensional antenna patterns applied to a cell sector that have a gain depending on the angle of arrival of the received signal. Three sectors per cell are specified.

### B. Related Work

In [8] the virtual center of a circular shaped cell is calculated, that is considered to be the source of UL interference power. The adjusted mean of interference power is used to calculate system capacity. In [9] this model is extended to hexagonally shaped, sectorized cells. Our work presented in [10] derives the UL interference power distribution of a single cell neglecting random shadow fading. In [11] the downlink (DL) interference power distribution is calculated using a method to approximate the sum distribution of multiple log-normally distributed interference power sources. The authors of [12] present a approximation to calculate the capacity of an LTE system under FFR.

In the following, we present a method to calculate the UL interference power distribution and there from the capacity and spectral efficiency under PFR. In Section II we develop an analytical model to calculate the uplink capacity based on the channel models introduced in Section I. Section III presents capacity and spectral efficiency results gained from this model. We conclude this work in Section IV and give an outlook on possible future extensions.

## II. CIR DISTRIBUTION CALCULATION

In a frequency reuse-1 scenario, received UL interference power can differ by orders of magnitude depending on the exact position of the interfering UT. Figure 2 shows a central hexagonal cell with one tier of interfering cells. Assuming equal transmission power $P_{TX}$, a UT at distance $d_{Imin} = R_x = \frac{\sqrt{3}}{2}R$ ($B_0$) would cause strongest mean interference. An UT at distance $d_{Imax} = \sqrt{(D + R_x)^2 + R_y^2}$ ($B_3$) with $R_y = \frac{R}{2}$ causes lowest interference. To determine the interference power distribution, the distribution of UTs at distance $d_I$ has to be derived. We assume UTs uniformly distributed in the area and an equal share of air time for each UT. At a given time instant, only one UT per cell is assumed active. The density of interferers at distance $d_I$ in one cell is

$$P(d_I) = \frac{l(d_I)dd_I}{A_{Hex}}. \tag{2}$$

$$y = \tau_z x + \nu_z, \tau_z x + \nu_z = \sqrt{d_I^2 - x^2} \tag{3}$$

As visible from Figure 2, $l(d_I) = d_I \alpha$ is the length of the arc of a circle with radius $d_I$ limited by the shape of the interfering cell and $A_{Hex} = \frac{3\sqrt{3}}{2}R^2$ is the total cell area. Angle $\alpha$ can be calculated as $2 \arctan \frac{y}{x}$. The point $[x; y]$ is the intersection of a circle of radius $d_I$ and a line through two vertices of the hexagon and can be calculated by solving Eq. (3) for positive $x$ and $y$. The factor $\tau_z$ is the slope and $\nu_z$ is the y-intersection of a line through two adjacent vertices $B_z, B_{z+1}$ of the hexagon. This way the five vertices split Eq. (2) into four continuous intervals. The last interval is limited by the line through $B_2, B_3$ and $B_3, B_4$ as shown in the dashed box on the right hand of Figure 2. The length of the arc $2d_I\alpha_-$ with $\alpha_- = \arctan \frac{y_-}{x_-}$ has to be subtracted.

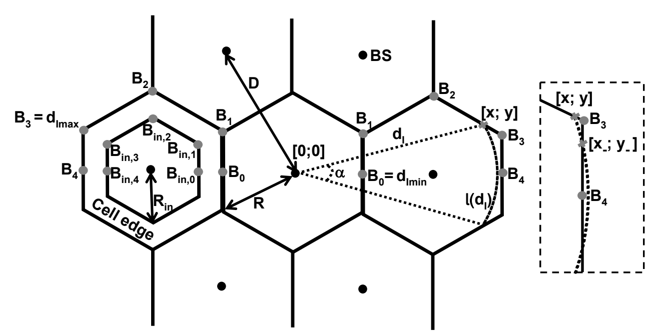


Fig. 2. Hexagonal scenario used to calculate the interference distance distribution.

Eq. (4) is used to derive the distance distribution of UTs at the cell edge under PFR. The angle $\alpha_{in}$ is calculated by previously used Eq. (3) but using the vertices $B_{in,z}$ of the inner (reuse-1) hexagon with area $A_{Hex,in}$. Equation (4) consists of nine continuous intervals, limited by the distances to the 10 different vertices.

$$P(d_I) = \frac{d_I\alpha - d_I\alpha_{in}}{A_{Hex} - A_{Hex,in}}. \quad (4)$$

The resulting probability distribution together with simulation results is shown in Figure 3 for the UMa scenario.

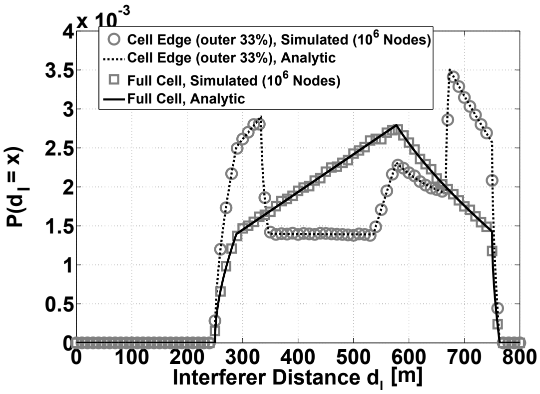


Fig. 3. Interferer distance distribution in the UMa scenario with and without PFR.

Antenna gains, e.g., sectorization is not considered in this model. To account for antenna gain, the length of the arc of equal received interference power, rather than just equal distance $d_I$, would have to be calculated.

Different from the channel model presented in [7], we do not consider interfering links to have LoS or NLoS propagation condition, chosen at random dependent on the distribution of distance of the UT from the BS. Instead we assume all interfering links to either have NLoS or LoS propagation conditions resulting in the respective maximum or minimum possible capacity of the network. Accordingly, we provide results for both limiting cases together. To estimate the error made by our assumption, the NLoS probability $P_{NLoS}(d_{Imin})$ for the closest possible interferer at distance $d_{Imin}$ is calculated using equations specified in [7] to be 76.9%, 91.1%, 57.5%, and 96.0% in UMi, UMa, RMa, and SMa scenarios, respectively. From this we can conclude, except for the RMa scenario, that calculated maximum possible capacity (only NLoS interference) must be close to the capacity obtained if random interference propagation conditions are applied.

All received interference power emitted at distance $d_I$ is assumed independent identically distributed (i.i.d.) following normal distribution with mean $\mu = P_{TX} - (\beta + \gamma \ln d_I)$ and standard deviation $\sigma$. The values for each IMT-A scenario are given in Table I. The conditional interference power probability density function (PDF) at distance $d = d_I$ is given by Eq. (1). The unconditional PDF is:

$$p(x_I) = \int_{d_{Imin}}^{d_{Imax}} P(d_I = d) p(x|d_I = d)) dd \quad (5)$$

which to our best knowledge has no closed form solution. What can be solved is an integral of the form

$$p(x_I) = \int_{d_{Imin}}^{d_{Imax}} \sum_{n=0}^{k} a_n d^n p(x|d_I = d)) dd \quad (6)$$

useful to solve for $p(x_I)$ with $P(d_I)$ approximated by a polynom of degree $k$ for each of the nine intervals $i$ of $P(d_I)$ introduced earlier. The approximation can be done using the least squares method. The approximated PDF of received interference power can be written as

$$p(x_I) = \sum_{i=1}^{9} (F(d_{Imax\_i}, i) - F(d_{Imin\_i}, i)), \quad (7)$$

$$\begin{aligned}
F(d_I, i) &= \int \sum_{n=0}^{k} a_{n,i} d^n p(x_I|d_I = d)) dd \\
&= \frac{1}{2\gamma} \Bigg( - a_{0,i} e^{\frac{-2\beta\gamma + \sigma^2 + 2\gamma(P_{TX} - x_I)}{2\gamma^2}} \\
&\mathrm{erf}\left( \frac{-\beta\gamma + \gamma P_{TX} + \sigma^2 - \gamma x_I - \gamma^2 \ln d_I}{\sqrt{2}\gamma\sigma} \right) + \\
&\sum_{n=1}^{k} \Bigg( a_{n,i} e^{(n+1)\frac{-2\beta\gamma + (n+1)\sigma^2 + 2\gamma(P_{TX} - x_I)}{2\gamma^2}} \\
&\mathrm{erf}\left( \frac{\beta\gamma - \gamma P_{TX} - (n+1)\sigma^2 + \gamma x_I + \gamma^2 \ln d_I}{\sqrt{2}\gamma\sigma} \right) \Bigg) \Bigg) \\
&+ const
\end{aligned}$$

The result for six interfering cells can be obtained after transform of Eq. (7) into linear domain and following convolution. We have not found a closed form solution, neither for the convolution integral nor for a transform to the frequency domain of this PDF. Instead, the method of *logarithmic convolution* [13] is used to get numeric results. Accordingly, if $X$ and $Y$ are random variables with known PDFs $p_x$ and $p_y$ the PDF $p_R$ of the random variable $R = 10\log_{10}(10^{\frac{X}{10}} + 10^{\frac{Y}{10}})$ is:

$$\begin{aligned}
p_R(r) &= \int_{-\infty}^{r} p_X(z) p_Y(D(r,z)) dz \\
&\quad + \int_{-\infty}^{r} p_X(D(r,z)) p_Y(z) dz, \quad (8) \\
D(r,z) &= 10\log_{10}(10^{\frac{r}{10}} - 10^{\frac{z}{10}})
\end{aligned}$$

The received carrier power of all UTs at distance $d_S$ is i.i.d. with normal distribution function with mean $\mu_S = P_{TX} - (\beta + \gamma \ln(d_S))$ and standard deviation $\sigma$ as defined in Table I. For the calculation of the distribution of the carrier signal power, the random selection of LoS and NLoS channel conditions (as specified in [7]) is considered. The LoS probability $P_{LoS}(d_S)$ depends on distance $d_S$ and is given in [7]. The NLoS probability $P_{NLoS}(d_S)$ is the complementary probability $P_{NLoS}(d_S) = 1 - P_{LoS}(d_S)$. Accordingly, the PDF of received carrier power at distance $d_S$ is a superposition

$$p(x_S|d_S) = \tag{9}$$
$$P_{LoS}(d_S)p(x_{S,LoS}|d_S) + (1 - P_{LoS}(d_S))p(x_{S,NLoS}|d_S)$$

The CIR distribution for UTs at distance $d_S$ can be calculated numerically through convolution, as shown in Eq. (10). The unconditioned distribution of the CIR is calculated numerically using Eq. (11).

$$p(x_{CIR}|d_S) = p(x_S|d_S) * p(-x_I) \tag{10}$$

$$p(x_{CIR}) = \int_{d_{Smin}}^{R} P(d_S = d)p(x_{CIR}|d_S = d)dd \tag{11}$$

The minimum distance $d_{Smin}$ from the Base Station (BS) is provided in [7] for each scenario. The ratio of terminals $P(d_S)$ at distance $d_S$ is calculated, analogical, to $P(d_I)$, see Eq. (2),(3). It is simplified to $\frac{2d_S}{A_{HexS}}, A_{HexS} = \frac{3\sqrt{3}}{2}R^2 - \pi d_{Smin}^2$ for $d_S < \frac{\sqrt{3}}{2}R$. If PFR is used, $P(d_S)$ needs to be refined to take reuse-1 inner cells and reuse-3 outer cells into account, see Eq. (4).

Assuming perfect link adaptation, the expected throughput can be derived directly from the CIR distribution function. For example values in Table II (taken from the 802.16-2009 standard [14]) together with Eq. (12) can be used to calculate mean throughput $\bar{r}$ where $m \leq M$ is the index of the MCS. The cell spectral efficiency can then be derived by normalizing to the bandwidth $B$ as given in Eq. (13).

$$\bar{r} = \sum_{m=1}^{M} r_m \int_{CIR_{min,m}}^{CIR_{min,m+1}} p(x_{CIR})dx_{CIR} \tag{12}$$

$$\eta = \frac{\bar{r}}{B} \tag{13}$$

TABLE II
IEEE 802.16 MCS AT 20 MHZ BANDWIDTH, FFT SIZE 2048, 192 PILOT SUB-CARRIERS, 1/8 CYCLIC PREFIX [14].

| m | MCS | $CIR_{min}$ [dB] | PHY Data Rate $r$ [Mbps] |
|---|---|---|---|
| 0 | None | $-\infty$ | 0 |
| 1 | QPSK $\frac{1}{2}$ | 5 | 14.93 |
| 2 | QPSK $\frac{3}{4}$ | 8 | 22.40 |
| 3 | 16QAM $\frac{1}{2}$ | 10.5 | 29.86 |
| 4 | 16QAM $\frac{3}{4}$ | 14 | 44.80 |
| 5 | 64QAM $\frac{1}{2}$ | 16 | 44.80 |
| 6 | 64QAM $\frac{2}{3}$ | 18 | 59.73 |
| 7 | 64QAM $\frac{3}{4}$ | 20 | 67.20 |
| 8 | | $\infty$ | |

## III. RESULTS

### A. Scenario and Assumptions

For the following results, Eq. (7) is used with $k = 1$. Approximations of Eq. (5) with $k > 1$ did not show significantly different results so that $k = 1$ is a sufficient choice. For all numerical integrations, summations of step size 0.1 m for distances, 0.1 dBm for powers, and 0.1 dB for ratios are used, MCSs and CIR related switching points are taken from Table II. The data rate was scaled proportionally if less than $B = 20$ MHz channel bandwidth is used. This means the data rate for the center band is scaled by $\alpha$, and for the edge band by $\frac{1-\alpha}{3}$ because of reuse-3 for cell edge areas, with $\alpha = \frac{R_{in}^2}{R^2}$ the ratio of the center cell to cell edge area.

A slow shadow fading process is assumed, permitting the scheduler to predict available throughput when choosing a MCS for a link to be served. What cannot be predicted is the interference power variance resulting from random UT active in interfering cells.

### B. CIR Results

Figure 4 presents the CIR Cumulative Distribution Function (CDF) experienced by UTs at distance $R/2$ when served with LoS channel condition by their serving BS and NLoS channel conditions to interfering nodes in the UMi scenario. Random shadow fading is not taken into account.

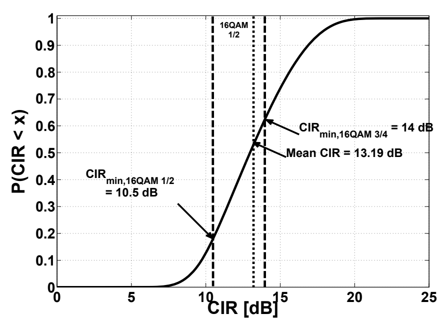


Fig. 4. CIR CDF experienced by a UT at distance $d_S = R/2$ with LoS channel to its serving BS. Scenario: UMi

CIR under NLoS interference, ranges from 2.6 dB to 21.6 dB and therefore all MCSs are needed. The mean CIR is 13.19 dB evaluated to MCS 16QAM 1/2. Assuming this MCS to be used throughout (without link adaptation) would result in 17% under- and 37% overestimation of the channel quality. It appears reasonable to measure and take into account the CIR variance before selecting a MCS. Alternatively, a scheduler could apply more robust MCSs keeping some target error rate as constraint.

To reduce the impact of CIR variance on system throughput the method described in [10] could be applied, namely schedule terminals from approximately the same area in the same recurring frequency-time resource, only. In the following we assume coordination across BSs to be possible, allowing all BS schedulers to select an appropriate MCS, taking into account knowledge which interfering UTs of the surrounding cells are scheduled at which frequency-time resource.

Figure 5 shows CIR CDF for reuse distance one. For verification, results from Monte Carlo simulation with approximately one million nodes per cell are shown for the NLoS interference case. If the required CIR for the most

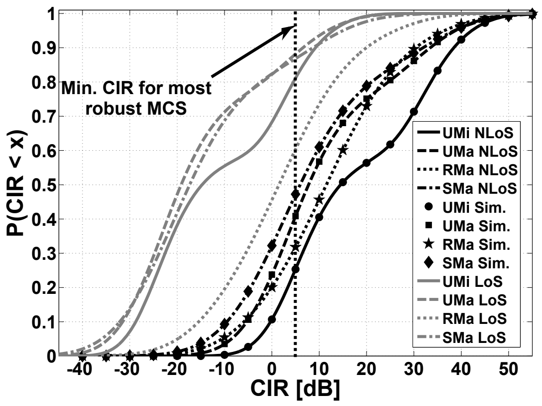


Fig. 5. CIR CDF for reuse distance one.

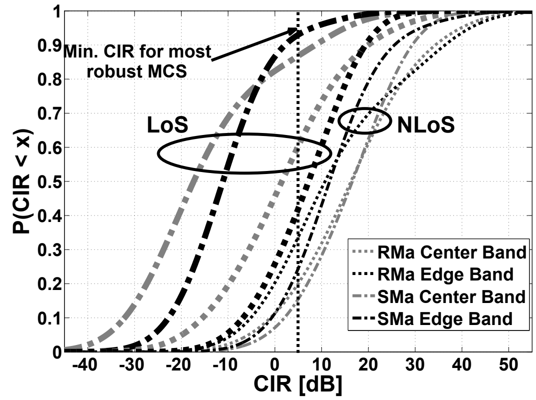


Fig. 7. CIR CDF of center- and edge band for RMa and SMa scenario, $\alpha = 2/3$.

robust MCS is 5 dB, system performance is very low. Results for the UMi scenario show best performance, but the outage probability is still 25% for NLoS and 80% for LoS interference power propagation conditions. RMa scenario has 32% and 60%, UMa $41\%$ and $87\%$, and SMa scenario has the highest outage probability of $48\%$ and $86\%$ for NLoS and LoS interference power propagation conditions, respectively. The respective capacity achieved is presented in Figure 8. The capacity of the UMi scenario is the highest ($38.20$ Mbps) under NLoS interference. The SMa scenario shows lowest capacity ($23.92$ Mbps). If the channel to the interfering nodes has LoS propagation conditions, the capacity is significantly lower. Then the RMa scenario has highest capacity because of its high interference power attenuation due to the high inter-site distance. A further look at intermediate results shows that one key factor influencing performance is the probability of LoS service by the BS. The expected ratio of UTs with LoS channel condition to their serving BS is $\int_{d_{S_{min}}}^{R} P(d_S = d) P_{LoS}(d) dd$. This results in a LoS probability of $15\%$ in the SMa, $20\%$ in the UMa, $40\%$ in the UMi, and $56\%$ in the RMa scenario, respectively.

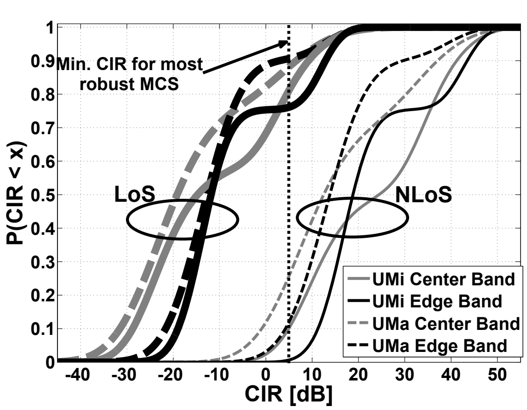


Fig. 6. CIR CDF of center- and edge band for UMi and UMa scenario, $\alpha = 2/3$.

Figures 6 and 7 show the CIR CDFs of the four scenarios if PFR is applied. The ratio $\alpha$ is kept fixed at $\alpha = 2/3$. The CIR distribution, compared to reuse-1, for all scenarios is improved and the outage probability decreased. Figure 8 compares the achieved capacity with and without PFR. The improved CIR with PFR under LoS propagation conditions for interfering links does not result in increased capacity. CIR is mainly improved in a region where no throughput is achieved anyways. Partitioning resources between three cells in the edge band leads to an overall decreased capacity, compared to the reuse-1 case. For NLoS channel propagation conditions of interfering links the partitioning of frequency spectrum resources to edge cells of three adjacent cells only results in a slight improvement of capacity by PFR. The capacity for the UMi, and RMa scenario is even decreased by PFR.

Figure 9 shows the spectral efficiency per cell calculated from Eq. (13). Results are presented for reuse-1 and PFR and compared to the minimal IMT-A requirements specified in [7]. In the following only results for NLoS propagation conditions of interfering links are discussed. The IMT-A requirements for the UMi scenario are met even under reuse-1 configuration. For UMa the requirement is slightly missed. Small time scale fading has not been considered in our model. RMa is a high speed scenario, where small time scale fading has a significant impact, while UMi and UMa will much less be impacted.

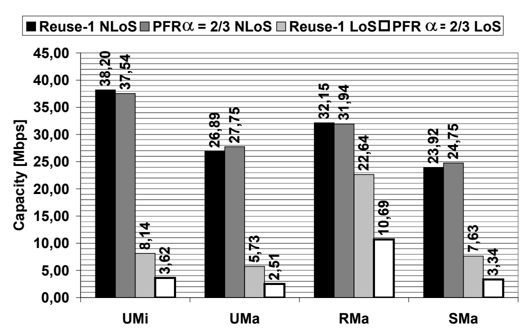


Fig. 8. Capacity with frequency reuse one and PFR.

Figure 10 shows the impact of the center- to edge band area ratio $\alpha$ on capacity. For NLoS propagation conditions

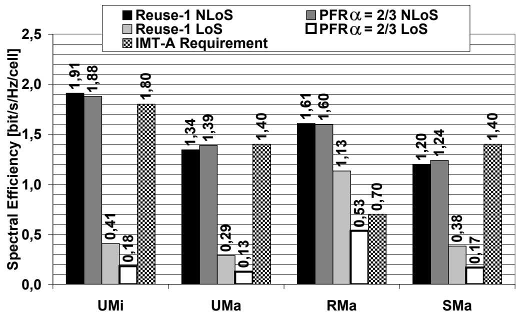


Fig. 9. Achieved and required spectral efficiency.

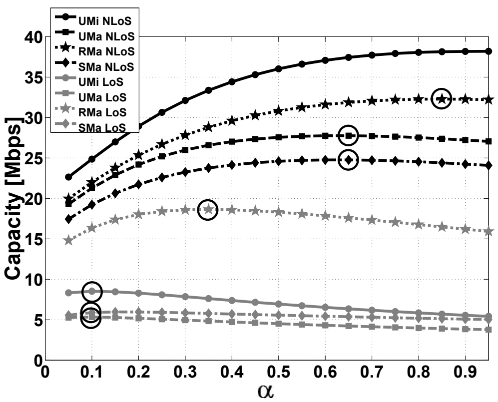


Fig. 10. Capacity for different ratios $\alpha$.

of interfering links the UMi scenario capacity increases as $\alpha$ increases. Maximum capacity of the UMi scenario is therefore reached in a reuse-1 configuration. The UMa and SMa scenarios show maximal capacity around $\alpha = 0.65$. The results presented in Figure 8 and Figure 9 are therefore very close to the maximal capacity that can be achieved in these scenarios. The RMa scenario reaches maximal capacity for $\alpha = 0.85$.

Under LoS interference power propagation conditions, all scenarios show better performance when approaching reuse-3 configuration. For the UMi, UMa, and SMa scenarios a slight capacity increase is achieved if approximately 10% of the cell area in the center are reserved for reuse-1 operation. Capacity of the RMa scenario is maximized if approximately 35% of the cell area in the center is reserved for reuse-1 operation.

## IV. Conclusion and Future Work

An analytic model is presented for calculating UL spectral efficiency of OFDMA based cellular networks with arbitrary UT deployments taking random LoS and NLoS channel condition for the serving BS channel, Fractional Frequency Reuse (FFR), and log-normal shadow fading into account. The model is applied to evaluate IEEE 802.16 systems for IMT-A evaluation scenarios. The results show, that the UL performance is very poor in reuse-1 deployments without spatial multiplexing support.

FFR in a version known as Partial Frequency Reuse (PFR) [4] is shown to provide a slight performance increase under NLoS interference channel propagation conditions in some IMT-A scenarios, but even lower performance in the Urban Microcell scenario. The model introduced in this paper can be used to calculate the optimal fraction of radio resources to be assigned to cell edge and to cell center, respectively. The minimum cell edge user spectral efficiency, which is another IMT-A evaluation requirement, can also be calculated using our method.

The model is currently not capable to represent a random choice of LoS and NLoS channel propagation condition for interfering nodes and is therefore not applicable to the IMT-A Rural Macro scenario, which has a high probability of LoS propagation for interfering nodes. For the future it is planed to take a varying transmission power into account to be able to study the contribution of more advanced FFR algorithms, including Soft Frequency Reuse (SFR), on system performance.

## References

[1] "IEEE 802.16m System Description Document," IEEE, Piscataway, NJ, 2009.

[2] "Evolved Universal Terrestrial Radio Access (E-UTRA) and Evolved Universal Terrestrial Radio Access Network (E-UTRAN); Overall description ," 3GPP, Tech. Rep. 3GPP 36.300, September 2009.

[3] Y. Xiang, J. Luo, and C. Hartmann, "Inter-cell Interference Mitigation through Flexible Resource Reuse in OFDMA based Communication Networks," in *13th European Wireless Conference EW2007*, 2007.

[4] M. Sternad, T. Ottosson, A. Ahlen, and A. Svensson, "Attaining both Coverage and High Spectral Efficiency with Adaptive OFDMA Downlinks," in *IEEE Vehicular Technology Conference*, vol. 4. Citeseer, 2003, pp. 2486–2490.

[5] Z. Xie and B. Walke, "Enhanced Fractional Frequency Reuse to Increase Capacity of OFDMA Systems," in *Proceedings of the 3rd International conference on New Technologies, Mobility and Security (NTMS 2009)*, 2009.

[6] M. Bohge, J. Gross, and A. Wolisz, "Optimal Power Masking in Soft Frequency Reuse Based OFDMA Networks," in *Proc. of the European Wireless Conference 2009, pages=162–166, year=2009*.

[7] "Guidelines for Evaluation of Radio Interface Technologies for IMT-Advanced," ITU-R, Tech. Rep. ITU-R M.2135, November 2008.

[8] J. Habetha and J. Wiegert, "Network Capacity Optimisation, Part 1: Cellular Radio Networks," in *Proceedings of 10th Symposium on Signal Theory, Aachen*, 2001, pp. 125–132.

[9] C. Hoymann and S. Goebbels, "Dimensioning Cellular WiMAX Part I: Singlehop Networks," in *Proceedings of 13th European Wireless Conference*, 2007.

[10] M. Mühleisen, B. Wolz, M. Siddique, and C. Görg, "Capacity Analysis and Improvement for Coexisting IEEE 802.16 Systems in Unlicensed Spectrum," in *Proceedings of 20th IEEE International Symposium on Personal, Indoor and Mobile Radio Communications (PIMRC 09)*, Tokyo, Japan, 2009.

[11] J. Wu, N. Mehta, and J. Zhang, "Flexible Lognormal Sum Approximation Method," in *Proc. IEEE Globecom 2005*, 2005, pp. 3413–3417.

[12] Huawei, "Soft Frequency Reuse Scheme for UTRAN LTE," 3GPP, Tech. Rep. R1-050507, 2005.

[13] J. Punt and D. Sparreboom, "Summing Received Signal Powers with Arbitrary Probability Density Functions on a Logarithmic Scale," *Wireless Personal Communications*, vol. 3, no. 3, pp. 215–224, 1996.

[14] *IEEE Std 802.16-2009, IEEE Standard for Local and Metropolitan Area Networks. Part 16: Air Interface for Fixed and Mobile Broadband Wireless Access Systems*, IEEE Std., 2009.